Inorg. Chem. **2008**, *47*, 7802−7812

Remarkable Tuning of the Photophysical Properties of Bifunctional Lanthanide tris(Dipicolinates) and its Consequence on the Design of Bioprobes

Anne-Laure Gassner, Céline Duhot, Jean-Claude G. Bünzli,* and Anne-Sophie Chauvin*

École Polytechnique Fédérale de Lausanne, Laboratory of Lanthanide Supramolecular Chemistry, BCH 1405, CH-1015 Lausanne, Switzerland

Received May 8, 2008

Derivatives of dipicolinic acid with a polyoxyethylene pendant arm at the pyridine 4-position have been functionalized for potential grafting with biological material. Four ligands with different terminal functions (alcohol, methoxy, phtalimide and amine) have been synthesized, which react with trivalent lanthanide ions Ln^{III} to yield triple helical $[Ln(L)_3]^{3-}$ complexes, as shown by NMR and UV−vis titrations. The tris chelates display large thermodynamic stability with log $\beta_{13} \approx 19-20$ for all Eu^{III} complexes for instance. Photophysical measurements reveal adequate sensitization of the metal-centered luminescence in the europium ($\eta_{sens} = 33-72\%$) and terbium complexes, which is modulated by the nature of the terminal function. The lifetimes of the metal-centered excited states are long, up to 1.4 ms for $[Eu(L)_3]^{3-}$ and 1.6 ms for $[Tb(L)_3]^{3-}$ at room temperature, in line with hydration numbers essentially equal to zero. Quantum yields are as high as 29% for the $[Eu(\mathbf{L^{NH2}})_3]^{3-}$ and 18% for the $[Tb(\mathbf{L^{OH}})_3]^{3-}$ tris chelates in water at physiological pH. These series of complexes demonstrate the extent of fine-tuning achievable for lanthanide luminescent probes and are simple models for investigating the effect of binding to biological molecules on the metal-centered luminescent properties.

Introduction

Probing and sensing intracellular biological analytes and events is of utmost importance for medical diagnosis and drug development, so that numerous attempts are being conducted to develop highly sensitive optical probes.[1–3] Lanthanide chelates are representing a growing share of the latter[4–6] due to their unique luminescent properties, sharp emission lines, and long lifetimes of the excited states allowing the use of time-resolved detection.[7,8] Furthermore, lanthanide complexes do not suffer much from the photobleaching problems encountered with organic dyes because Ln^{III} ions are efficient quenchers of triplet states. Sensitive intracellular biological analyses require optical probes that are water soluble, thermodynamically stable and kinetically inert at physiological pH, cell permeable, and nontoxic, in addition to possessing adequate luminescent properties. A great deal of knowledge has been accumulated during the last decades to meet these stringent requirements.[9] A further critical point is to tailor a probe targeting a given analyte or binding to a specific organelle of a living cell. This can be achieved through binding to an antigen or a protein, after activation of the coupling function of the probe or upon interaction of the chelate with an activated target. Another strategy is to synthesize a complex having one extremity fitted with a receptor specific for the targeted biological molecule or analyte, which implies a coupling reaction with the receptor after activation of either the probe or the receptor. Ideally, the complex acting as a probe should be simple and easy to synthesize; one strategy consists therefore

* To whom correspondence should be addressed. E-mail: jean-claude.bunzli@epfl.ch (J.-C.G.B); anne-sophie.chauvin@epfl.ch (A.-S.C.).

(1) Johnsson, N.; Johnsson, K. *ACS Chem. Biol.* **2007**, *2*, 31–38.
(2) Miller, E. W.; Bian, S. X.; Chang, C. J. *J. Am. Chem. Soc.* **2007**, *129*, 3458–3459.
(3) Du, W.; Wang, Y.; Luo, Q.; Liu, B. F. *Anal. Bioanal. Chem.* **2006**, *386*, 444–457.
(4) Martin, L. J.; Hahnke, M. J.; Nitz, M.; Wohnert, J.; Silvaggi, N. R.; Allen, K. N.; Schwalbe, H.; Imperiali, B. *J. Am. Chem. Soc.* **2007**, *129*, 7106–7113.
(5) Poole, R. A.; Montgomery, C. P.; New, E. J.; Congreve, A.; Parker, D.; Botta, M. *Org. Biomol. Chem.* **2007**, *5*, 2055–2062.
(6) Pal, R.; Parker, D. *Org. Biomol. Chem.* **2008**, *6*, 1020–1033.
(7) Bünzli, J.-C. G.; Piguet, C. *Chem. Soc. Rev.* **2005**, *34*, 1048–1077.
(8) Bünzli, J.-C. G. *Acc. Chem. Res.* **2006**, *39*, 53–61.
(9) Gunnlaugsson, T.; Stomeo, F. *Org. Biomol. Chem.* **2007**, *5*, 1999–2009.

10.1021/ic800842f CCC: $40.75
Published on Web 07/26/2008

in turning to existing chelating agents the properties of which are well established and which lend themselves to easy derivatization.

Dipicolinic acid (H_2dpa) is one of such potential chelating units. It is known to form stable anionic $[Ln(dpa)_3]^{3-}$ complexes with lanthanide ions[10,11] at physiological pH. Numerous crystal structures have been reported,[12–15] showing the influence of the counterion on the triple helical structure with idealized D_3 symmetry. The solution structures of the $[Ln(dpa)_3]^{3-}$ chelates and corresponding complexes with derivatized dipicolinates are close to the solid-state structures, as unraveled by analysis of the lanthanide-induced shifts (LIS).[16–19] Although the tris complexes exist as racemic mixtures of Λ or Δ isomers, their optical activity is well understood[20–23] as well as the one of mixed complexes with chiral ligands. The luminescent complexes can thus be used for chirality recognition by perturbing the racemic equilibrium with enantiomerically resolved nonluminescent acceptor molecules or complexes.[24] The parent $[Ln(dpa)_3]^{3-}$ chelates with Eu^{III} and Tb^{III} display intense luminescence, thanks to sensitization through the dpa^{2-} triplet state[25] with an efficiency of 85% for the tris complex in the solid state[26] and of 61% in solution.[27] These chelates have been proposed as secondary standards for quantum yield determination.[27] The effect of substituents grafted on the pyridine 4-position on the emission intensity is documented both for Tb^{III} [28–30] and Eu^{III} (together with the role of 3,5 substituents).[31] Near-infrared luminescence from Nd^{III}, Dy^{III}, Er^{III}, Tm^{III}, and Yb^{III} is also sensitized by dipicolinate moieties[18,32,33] although usually to a lesser extent than visible emission. These remarkable luminescent properties have led to introduce lanthanide dipicolinates into various inorganic−organic hybrid materials[34] or nanoparticles,[35] as well as to provide them as analytical probes, particularly for the analysis of bacterial spores[36–38] or of nanomolar concentrations of Tb^{III}.[39] They are also the active components of a bar-code system bearing more information than the conventional ones.[40] Finally, the lanthanide dipicolinates display nonlinear optical (NLO) properties[41,42] and two-photon excitation luminescence, either through an allowed Tb^{III} f−f transition[43] or through the ligand,[44,45] enabling luminescence microscopy images to be collected under NIR excitation. The latter property is a real advantage for bioprobes because dipicolinates have absorption maxima around 270−300 nm, a spectral range detrimental to living materials.

The simple dipicolinates cannot however be coupled directly to biological molecules. Therefore derivatives with substitution at the 4-position of the pyridine ring have been designed.[28,31,46–50] Building on our successful strategy for bimetallic helicates,[51–55] we have grafted a polyoxyethylene substituent in this position, which bears various terminal groups (Scheme 1) for potential coupling with biological material. Two of the ligands have protic terminal functions, alcohol and amine, whereas the two other ones bear protected functions, methoxy, and phtalimide. The properties of the

(10) Grenthe, I. *J. Am. Chem. Soc.* **1961**, *83*, 360–364.
(11) Grenthe, I. *Acta Chem. Scand.* **1963**, *17*, 2487.
(12) Mondry, A.; Starynowicz, P. *J. Alloys Compd.* **1995**, *225*, 367–371.
(13) Harrowfield, J. M.; Kim, Y.; Skelton, B. W.; White, A. H. *Aust. J. Chem.* **1995**, *48*, 807–823.
(14) Brayshaw, P. A.; Bünzli, J.-C. G.; Froidevaux, P.; Harrowfield, J. M.; Kim, Y.; Sobolev, A. N. *Inorg. Chem.* **1995**, *34*, 2068–2076.
(15) Brayshaw, P. A.; Harrowfield, J. M.; Sobolev, A. N. *Acta Crystallogr., Sect. C* **1995**, *51*, 1799–1802.
(16) Donato, H.; Martin, R. B. *J. Am. Chem. Soc.* **1972**, *94*, 4129–4131.
(17) Reilley, C. N.; Good, B. W.; Desreux, J. F. *Anal. Chem.* **1975**, *47*, 2110–2116.
(18) Platas, C.; Piguet, C.; André, N.; Bünzli, J.-C. G. *J. Chem. Soc., Dalton Trans.* **2001**, 3084–3091.
(19) Ouali, N.; Bocquet, B.; Rigault, S.; Morgantini, P.-Y.; Weber, J.; Piguet, C. *Inorg. Chem.* **2002**, *41*, 1436–1445.
(20) Das Gupta, A.; Richardson, F. S. *Inorg. Chem.* **1981**, *20*, 2616.
(21) Coruh, N.; Hilmes, G. L.; Riehl, J. P. *Inorg. Chem.* **1988**, *27*, 3647–3651.
(22) Hopkins, T. A.; Bolender, J. P.; Metcalf, D. H.; Richardson, F. S. *Inorg. Chem.* **1996**, *35*, 5356–5362.
(23) Hopkins, T. A.; Bolender, J. P.; Metcalf, D. H.; Richardson, F. S. *Inorg. Chem.* **1996**, *35*, 5347–5355.
(24) Aspinall, H. C. *Chem. Rev.* **2002**, 1807–1850.
(25) Prendergast, F. G.; Lu, J.; Callahan, P. J. *J. Biol. Chem.* **1983**, *258*, 4075–4078.
(26) Gumy, F.; Bünzli, J.-C. G. 2008, unpublished results.
(27) Chauvin, A.-S.; Gumy, F.; Imbert, D.; Bünzli, J.-C. G. *Spectrosc. Lett.* **2004**, *37*, 517–532, erratum, 2006, **40**, 193.
(28) Lamture, J. B.; Zhou, Z. H.; Kumar, A. S.; Wensel, T. G. *Inorg. Chem.* **1995**, *34*, 864–869.
(29) Yin, X.-H.; Tan, M. Y. *Zhongguo Xitu Xuebao (J. Chin. Rare Earth Soc.)* **2001**, *19*, 555–560.
(30) Yin, X.-H.; Yang, M. Y.; Shi, H. H.; Yang, G.; Chen, X. B.; Gu, L.-Q. *Zhongguo Xitu Xuebao (J. Chin. Rare Earth Soc.)* **2000**, *18*, 211–214.
(31) George, M. W.; Golden, C. A.; Grossel, M. C.; Curry, R. J. *Inorg. Chem.* **2006**, *45*, 1739–1744.
(32) Yang, W.; Gao, J. Z.; Chen, M.; Kang, J. W. *Spectrosc. Lett.* **1997**, *30*, 367–378.
(33) Reinhard, C.; Güdel, H. U. *Inorg. Chem.* **2002**, *41*, 1048–1055.
(34) Lai, D. C.; Dunn, B.; Zink, J. I. *Inorg. Chem.* **1996**, *35*, 2152–2154.
(35) Soares-Santos, P. C. R.; Nogueira, H. I. S.; Felix, V.; Drew, M. G. B.; Ferreira, R. A. S.; Carlos, L. D.; Trindade, T. *Chem. Mater.* **2003**, *15*, 100–108.
(36) Pellegrino, P. M.; Fell, N. F.; Rosen, D. L.; Gillespie, J. B. *Anal. Chem.* **1998**, *70*, 1755–1760.
(37) Cable, M. L.; Kirby, J. P.; Sorasaenee, K.; Gray, H. B.; Ponce, A. *J. Am. Chem. Soc.* **2007**, *129*, 1474–1475.
(38) Kirby, J. P.; Venkateswaran, K. J.; Ponce, A. U.S. Patent 7,306,930, 2007.
(39) Barela, T. D.; Sherry, A. D. *Anal. Biochem.* **1976**, *71*, 351–357.
(40) Auslander, J. D.;. Berson, W. *U.S. Patent 5,542,971,* 1996.
(41) Tancrez, N.; Feuvrie, C.; Ledoux, I.; Zyss, J.; Toupet, L.; Le Bozec, H.; Maury, O. *J. Am. Chem. Soc.* **2005**, *127*, 13474–13475.
(42) Hou, H.; Wei, Y.; Song, Y.; Fan, Y.; Zhu, Y. *Inorg. Chem.* **2004**, *43*, 1323–1327.
(43) D'Aléo, A.; Pompidor, G.; Elena, B.; Vicat, J.; Baldeck, P. L.; Toupet, L.; Kahn, R.; Andraud, C.; Maury, O. *ChemPhysChem* **2007**, *8*, 2125–2132.
(44) Picot, A.; Malvolti, F.; LeGuennic, B.; Baldeck, P. L.; Williams, J. A. G.; Andraud, C.; Maury, O. *Inorg. Chem.* **2007**, 2659–2665.
(45) Picot, A.; D'Aleo, A.; Baldeck, P. L.; Grichine, A.; Duperray, A.; Andraud, C.; Maury, O. *J. Am. Chem. Soc.* **2008**, *130*, 1532–1533.
(46) Latva, M.; Takalo, H.; Mukkala, V. M.; Matachescu, C.; Rodriguez-Ubis, J.-C.; Kankare, J. *J. Lumin.* **1997**, *75*, 149–169.
(47) Lamture, J. B.; Wensel, T. G. *Tetrahedron Lett.* **1993**, *34*, 4141–4144.
(48) Lamture, J. B.; Iverson, B.; Hogan, M. E. *Tetrahedron Lett.* **1996**, *37*, 6483–6486.
(49) Lamture, J. B.; Wensel, T. G. *Bioconjugate Chem.* **1995**, *6*, 88–92.
(50) Muller, G.; Schmidt, B.; Jiricek, J.; Hopfgartner, G.; Riehl, J. P.; Bünzli, J.-C. G.; Piguet, C. *J. Chem. Soc., Dalton Trans.* **2001**, 2655–2662.
(51) Vandevyver, C. D. B.; Chauvin, A.-S.; Comby, S.; Bünzli, J.-C. G. *Chem. Commun.* **2007**, 1716–1718.
(52) Chauvin, A.-S.; Comby, S.; Song, B.; Vandevyver, C. D. B.; Bünzli, J.-C. G. *Chem.—Eur. J.* **2007**, *13*, 9515–9526.
(53) Chauvin, A.-S.; Comby, S.; Song, B.; Vandevyver, C. D. B.; Bünzli, J.-C. G. *Chem.—Eur. J.* **2008**, *14*, 1726–1739.
(54) Bünzli, J.-C. G.; Chauvin, A.-S.; Vandevyver, C. D. B.; Song, B.; Comby, S. *Ann. N. Y. Acad. Sci.* **2008**, *1130*, 97–105.
(55) Deiters, E.; Song, B.; Chauvin, A.-S.; Vandevyver, C. D. B.; Bünzli, J.-C. G. *New J. Chem.* **2008**, *32* (7), 1140–1152.

Scheme 1

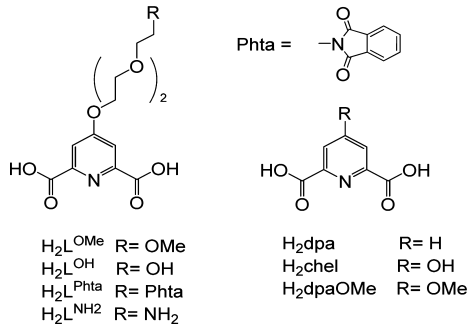

$[Ln(\mathbf{L^{OH}})_3]^{3-}$ and $[Ln(\mathbf{L^{NH2}})_3]^{3-}$ tris chelates are presented and compared to those of the complexes bearing a protected group, $[Ln(\mathbf{L^{OMe}})_3]^{3-}$ and $[Ln(\mathbf{L^{Phta}})_3]^{3-}$.

Synthesis of the Ligands. The synthesis of ligands $H_2\mathbf{L^{OMe}}$ and $Na_2\mathbf{L^{OH}}$ starts from diester **2** onto which the polyoxyethylene pendant arm is grafted by means of a Mitsunobu reaction (Scheme 2). Using the commercial 2-[2-(2-methoxy-ethoxy)-ethoxy]-ethanol reactant gives diester **4**, which can be directly hydrolyzed into $H_2\mathbf{L^{OMe}}$; the three-step synthesis has an overall yield of 57%. Ligand $Na_2\mathbf{L^{OH}}$ is obtained via a four-step synthesis with an overall yield of 45% by removing the ether function of **4** in presence of iodotrimethylsilane and hydrolysis of the resulting alcohol **5**. For the other two ligands, the polyoxyethylene arm bearing a terminal methoxy function is first introduced onto a phthalimide group via a Mitsunobu reaction. Removal of the methoxy group results in alcohol **7**, which provides diester **8** thanks to a second Mitsunobu reaction. Depending on the hydrolysis conditions used for the latter, either $H_2\mathbf{L^{NH2}}$ or $Na_2\mathbf{L^{Phta}}$ is isolated. An ethanolic solution of sodium hydroxide at ambient temperature only hydrolyzes the ester moieties, leading to $Na_2\mathbf{L^{Phta}}$ with an overall yield of 50%. Isolating $\mathbf{L^{NH2}}$ proved to be more difficult: the removal of phthalimide is classically carried out in presence of monohydrate hydrazine, here concomitant with the hydrolysis of the diester functions. However, under these experimental conditions, an intermediate product formed, possibly a hydrazone derivative, which could not be separated from the expected ligand. Consequently, we used an excess of aqueous sodium hydroxide at 40 °C and isolated $H_2\mathbf{L^{NH2}}$ by chromatography (overall yield 47%). This ligand decomposes if the solid is dried under vacuum at a temperature higher than 40 °C so that it has to be handled with care. The four isolated ligands are water soluble whatever the pH is, so that they cannot be purified by crystallization. Purification, particularly the removal of inorganic salts, was achieved by chromatography: silica phases ($MeCN/NH_4OH$) were used for $Na_2\mathbf{L^{OH}}$ and $Na_2\mathbf{L^{Phta}}$, whereas $H_2\mathbf{L^{OMe}}$ and $H_2\mathbf{L^{NH2}}$ required inverse-phase chromatography (C_{18} reverse phase, MeCN, H_2O, TFA). Depending on the purification conditions, the ligands were isolated either as carboxylic acids or as sodium salts.

Acidity Constants of the Ligands. The fully protonated form of the ligands possesses three deprotonation sites (two carboxylic acid functions, as well as a pyridinium nitrogen); in the case of $H_2\mathbf{L^{NH2}}$ a fourth deprotonation site is due to the presence of the terminal amine. Acidity constants were first determined by UV−vis spectrophotometric titrations in the spectral range 200−550 nm and pH range 1.1−12. The evolution of the absorption spectra of $\mathbf{H_2L^{OH}}$ is given in Figure 1 as an example (Figure S1 in the Supporting Information) for the other ligands. Experimental data were fitted to the set of eqs 1–3. In the case of ligands $\mathbf{H_2L^{OMe}}$ and $\mathbf{Na_2L^{Phta}}$, determination of the low pK_{a1} values had to be performed separately by measuring absorption spectra of solutions prepared from fuming HCl with calculated exact pH values in the range 0−2. The other pK_a values were determined by fitting the UV−vis spectra in the higher pH range. All obtained values are reported in Table 1.

$$(H_nL)^{(2-n)-} \overset{K_{a1}}{\rightleftharpoons} (H_{n-1}L)^{(3-n)-} + H^+ \qquad K_{a1} = \frac{[H_{n-1}L][H]}{[H_nL]} \tag{1}$$

$$(H_{n-1}L)^{(3-n)-} \overset{K_{a2}}{\rightleftharpoons} (H_{n-2}L)^{(4-n)-} + H^+ \qquad K_{a2} = \frac{[H_{n-2}L][H]}{[H_{n-1}L]} \tag{2}$$

$$(HL)^- \overset{K_{an}}{\rightleftharpoons} (L)^{2-} + H^+ \qquad K_{an} = \frac{[L][H]}{[HL]} \tag{3}$$

The first two acidity constants correspond to ionization of the carboxylic acid functions, and pK_{a3} to that of the pyridinium nitrogen, whereas the fourth value corresponds to the deprotonation of the ammonium group in $H_2\mathbf{L^{NH2}}$. The recalculated spectra of the different species are shown in Figure S2 in the Supporting Information, and extractions at different wavelengths in Figure S3 in the Supporting Information.

The pK_a assignments were subsequently substantiated by monitoring the evolution of the ^1H NMR spectra in D_2O as a function of pD. The chemical shifts of the pyridine protons as well as of proton H^1 of the polyoxyethylene substituent (Scheme 2 for the numbering scheme) are very sensitive to deprotonation of both the carboxylic acid and the pyridinium functions and are consequently ideal NMR probes (Figure 2 for $Na_2\mathbf{L^{OH}}$ and Figure S4 in the Supporting Information for the plot of chemical shifts vs pD for H_{py} and/or H^1). When plotting the chemical-shift values versus pD, three inflection points are detected, which correspond fairly well to the pK_a's reported in Table 1, taking into account the relationship pH = pD − 0.4.[58] Protons H^2 to H^6 are less sensitive to pH changes, but similar features can be observed. The same approach has been successfully applied to the other ligands, except for the pK_{a1} values of $H_2\mathbf{L^{OMe}}$ and $Na_2\mathbf{L^{Phta}}$. Interestingly, methoxy protons of $H_2\mathbf{L^{OMe}}$ and phtalimide aromatic protons of $Na_2\mathbf{L^{Phta}}$ proved to be pD sensitive despite that both ROESY experiments and CAChe predictions demonstrate that the functionalized polyoxyethylene arm adopts an extended configuration.

(56) Crans, D. C.; Yang, L. Q.; Jakusch, T.; Kiss, T. *Inorg. Chem.* **2000**, *39*, 4409–4416.
(57) Tichane, R. M.; Bennett, W. E. *J. Am. Chem. Soc.* **1957**, *79*, 1293–1296.
(58) Mikkelsen, K.; Nielsen, S. O. *J. Phys. Chem.* **1960**, *64*, 632–637.

Scheme 2

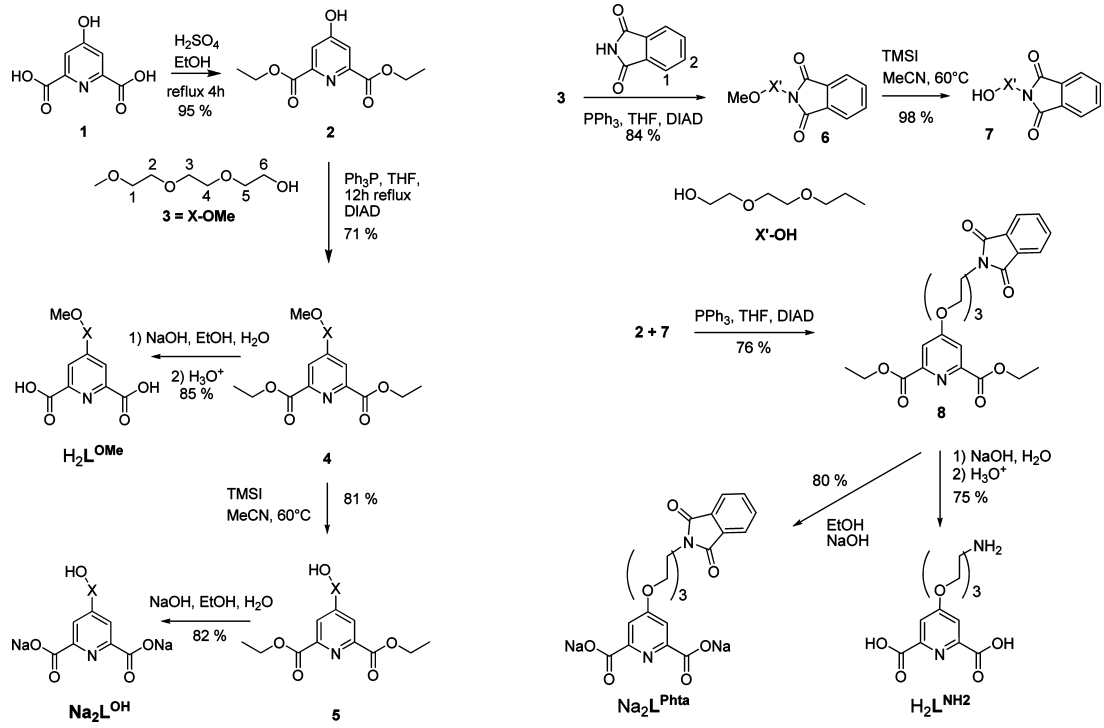

Comparing the pK_a values obtained for the four new ligands with those of dipicolinic acid reveals pK_{a2} and pK_{a3} being larger by more than two units. This is due to the linking of the oxygen atom onto the pyridine ring as demonstrated by the similar pK_a values obtained for the model compound **H2dpaOMe**. As far as pK_{a1} is concerned, we note that $\mathbf{H_2L^{OH}}$ and $\mathbf{H_2L^{NH2}}$ display values around 2 which are substantially larger than those obtained for the other two ligands and for the reference compounds (≈0.5). This could be due to hydrogen bonding with carboxylic acid functions through intermolecular interactions, decreasing the acidity of the carboxylic acid function.[59] On the other hand, replacing the methoxy group of **H2dpaOMe** with the polyoxyethylene chain in $\mathbf{H_2L^{OMe}}$ has no consequence on pK_{a1}. Distribution diagrams are presented in Figure S5 in the Supporting Information. It can be seen that the ligands are totally deprotonated (>95%) at physiological pH except in the case of $\mathbf{H_2L^{NH2}}$ for which $(\mathbf{L^{NH2}})^{2-}$ (70%) and $(\mathbf{HL^{NH2}})^{-}$ (30%) coexist at this pH.

Interaction with Trivalent Lanthanide Ions. We turned to UV−vis spectrophotometric titrations and ^{1}H NMR spectra to get insight into the stoichiometry and stability of the

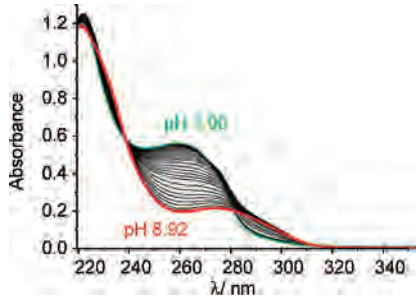

Figure 1. UV−vis absorption spectra of Na_2L^{OH} in the pH range 1.96 to 8.92; $[Na_2\mathbf{L^{OH}}]_t = 10^{-4}$ M, $T = 298$ K, $I = 0.1$ M (KCl).

Table 1. Acidity Constants of the Ligands from UV−vis Titration at 298 K, ($[L]_t = 10^{-4}$ M, $I = 0.1$ M KCl)

	$\mathbf{H_2L^{NH2}}$	$\mathbf{H_2L^{OH}}$	$\mathbf{H_2L^{OMe}}$	$\mathbf{H_2L^{Phta}}$	$\mathbf{H_2dpa}$[56a,57b]	**H2dpaOMe**
pK_{a1}	2.15 (12)	2.80 (4)	0.49 (9)	0.51 (8)	~ 0.5 (2)/−	0.9(5)
pK_{a2}	4.37 (10)	4.60 (4)	4.26 (3)	4.36 (2)	2.03 (1)/2.16	4.63(2)
pK_{a3}	5.77 (6)	6.09 (1)	6.03 (1)	6.24 (1)	4.49 (1)/4.76	6.37(1)
pK_{a4}	6.99 (6)					

[a] Ionic strength: 0.40. [b] At 303 K.

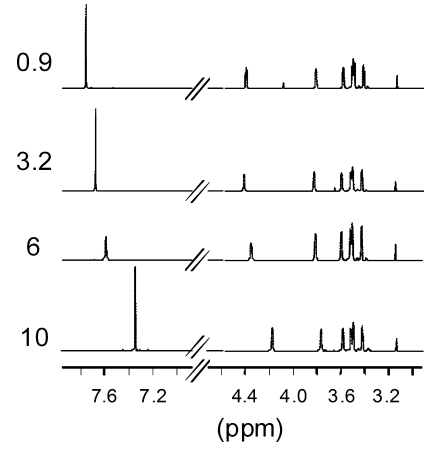

Figure 2. Evolution of the chemical shift of the aromatic protons of $\mathbf{Na_2L^{OH}}$ as a function of pD in D_2O; $[Na_2L^{OH}]_t = 4\eta 10^{-4}$ M.

lanthanide complexes formed with the four new ligands. Aqueous solutions 10^{-4} M of the latter, buffered at pH = 7.4, were titrated by $Ln(ClO_4)_3(H_2O)_x$ 10^{-3} M up to a ratio $R = [Ln^{III}]/[L]_t = 2.5$. The absorption spectra of the ligands are characterized by overlapping broad bands, assigned to n → π^* and π → π^* transitions, which are affected by complexation. Factor analysis points to three or four absorb-

(59) Huque, F. T. T.; Platts, J. A. *Org. Biomol. Chem.* **2003**, *1*, 1419–1424.

Table 2. Conditional Stability Constants Determined at 298 K and pH 7.4 in Tris−HCl 0.1 M, $I = 0.1$ M (KCl), $[L]_t = 10^{-4}$ M; Standard Deviations Are Given Within Parentheses

		La	Eu	Tb	Lu
$(\mathbf{L^{OMe}})^{2-}$	$\log \beta_{11}$	10.2 (6)	8.9	9.1 (6)	n.a.
	$\log \beta_{12}$	16.7 (8)	14.3 (2)	15.5 (6)	n.a.
	$\log \beta_{13}$	20.9 (7)	20.5 (2)	21.4 (6)	n.a.
$(\mathbf{L^{OH}})^{2-}$	$\log \beta_{11}$	7.9 (4)	8.8 (2)	8.7 (1)	8.8[b]
	$\log \beta_{12}$	14.2 (5)	15.1 (2)	15.1 (2)	16.6 (1)
	$\log \beta_{13}$	20.2(6)	20.3 (3)	20.3 (3)	22.8 (2)
$(\mathbf{L^{Phta}})^{2-}$	$\log \beta_{11}$	8.9[b]	8.9 [b]	8.9[b]	8.9[b]
	$\log \beta_{12}$	14.0 (1)	14.4 (4)	13.9 (1)	15.3 (1)
	$\log \beta_{13}$	18.7 (1)	18.8(2)	19.3 (1)	20.9 (1)
$(\mathbf{L^{NH2}})^{2-}$	$\log \beta_{11}$	7.2 (1)	6.8 (4)	n.a.	8.5 (3)
	$\log \beta_{12}$	12.9 (1)	14.7 (4)	n.a.	15.5 (4)
	$\log \beta_{13}$	17.6 (1)	20.5 (4)	n.a.	20.4 (4)
$(\mathbf{dpa})^{2-a}$	$\log \beta_{11}$	8.0(1)	8.8(1)	8.7(3)	9.0(6)
	$\log \beta_{12}$	13.8(1)	16.0(2)	16.1(4)	16.8(6)
	$\log \beta_{13}$	18.1(1)	21.5(2)	22.0(4)	21.5(6)

[a] From ref 10. [b] Value fixed, otherwise convergence was not reached.

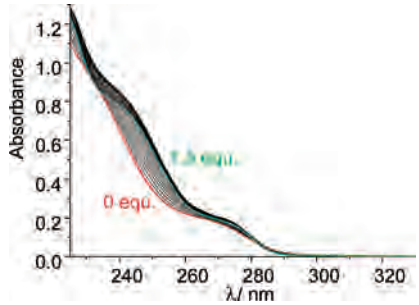

Figure 3. UV−vis absorption spectra of a solution of $(\mathbf{L^{NH2}})^{2-}$ in water (pH 7.4, Tris-HCl, $I = 0.1$ M KCl) upon addition of increasing amounts of La^{III}.

ing species in all cases, in line with the successive formation of complexes with 1:1, 1:2, and 1:3 stoichiometries. With the exception of some cases, data could be satisfactorily fitted to eqs 4–6, and the resulting stability constants are listed in Table 2, whereas Figure 3 presents the spectrophotometric titration of $(\mathbf{L^{NH2}})^{2-}$ with La^{III} as a typical example.

$$Ln^{3+} + (L)^{2-} \leftrightarrows [Ln(L)]^{+} \qquad \log \beta_{11} \qquad (4)$$

$$Ln^{3+} + 2(L)^{2-} \leftrightarrows [Ln(L)2]^{-} \qquad \log \beta_{12} \qquad (5)$$

$$Ln^{3+} + 3(L)^{2-} \leftrightarrows [Ln(L)3]^{3-} \qquad \log \beta_{13} \qquad (6)$$

These results point to the preferred formation of 1:3 complexes in aqueous solution with all the ligands and to a stability comparable to that of the complexes with $(dpa)^{2-}$,[60] with minor variations. Except for La^{III}, for which slightly more stable tris chelates are seemingly obtained with $(\mathbf{L^{OMe}})^{2-}$, $(\mathbf{L^{OH}})^{2-}$, and $(\mathbf{L^{NH2}})^{2-}$, the substitution in the pyridine 4-position leads to somewhat reduced stability, β_{13} being smaller by approximately 1 order of magnitude, taking uncertainties into account. Differences with respect to $[Ln(dpa)_3]^{3-}$ complexes are however often at the limit of significance and spectra of the various complexed species are heavily correlated (Figure S6 in the Supporting Information) so that a detailed discussion is pointless at this stage. The only useful conclusion is that the substitution and the

(60) Chauvin, A.-S.; Bernardinelli, G.; Alexakis, A. *Tetrahedron Asymmetry* **2006**, *17*, 2203–2209.

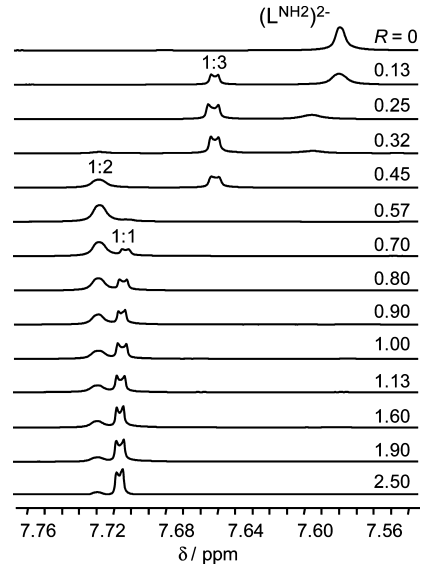

Figure 4. ^1H NMR spectra of the aromatic protons of the L^{NH2} ligand as a function of the ratio $R = [Lu^{III}]_t/[(L^{NH2})^{2-}]_t$, $[H_2L^{NH2}]_t = 4 \times 10^{-3}$ M in D_2O, pD 7.8, $T = 298$ K.

functionalization of the polyoxyethylene arm have little effect on the stability of the tris chelates.

To better substantiate the UV−vis data, ^1H NMR experiments were conducted in which 4×10^{-3} M solutions of each ligand in D_2O (pD = 7.8) were titrated by a 0.123 M $Lu(ClO_4)_3$ solution up to $R = [Lu^{III}]_t/[L]_t = 2.5$. The evolution of the ^1H NMR signals of the aromatic protons of $(\mathbf{L^{NH2}})^{2-}$ is depicted in Figure 4, whereas the spectral range corresponding to the protons of the polyoxyethylene substituent is shown in Figure S7 in the Supporting Information. In the uncomplexed ligand, the two aromatic protons of the pyridine moiety are equivalent ($\delta = 7.58$) on the NMR time scale. Upon addition of Lu^{III}, two down-shielded nonequivalent signals appear at an average value of 7.65 ppm, which are attributed to a 1:3 complex; non-equivalence can rise from the three ligand strands being not totally equivalent on the NMR time scale; furthermore, the resonance of the unbound ligand broadens and shifts downfield, indicating a ligand exchange reaction taking place.

When $R > 0.33$, the signal corresponding to the free ligand disappears completely and a new one assigned to the 1:2 species is seen at 7.72 ppm. The 1:1 species is observed for $R > 0.7$ along with the 1:2 species, which is still present for $R = 2.5$. The proportions of the complexed species determined by integration of the NMR signals can now be compared with predictions made using the stability constants reported in Table 2. At the concentration used for the NMR titration and for $R = 0.33$, one calculates the following speciation: 91% of the 1:3 chelate, 3.4% of the 1:2 species, and 5.7% of free ligand, which compares reasonably well with the NMR data: 84%, 6%, and 10%, respectively. Similar titrations have been conducted with the other ligands, leading to analogous observations; the chemical shifts of the different species are reported in Table 3. With respect to the free ligands L^{2-}, the chemical shifts of the pyridine protons remain small, in the range 0.09−0.15 ppm, except for $(\mathbf{L^{Phta}})^{2-}$ for which $\Delta\delta \leq 0.09$ ppm. Because the polyoxy-

Table 3. Chemical Shifts of the Free Ligands and Their Complexes $[Lu(L)_i]^{(3-2i)}$ ($i = 1-3$) in D_2O, $[L]_t = 4 \times 10^{-3}$ M, pD 7.8, $T = 298$ K

		H^{py}	H^1	H^2	$H^{3,4}$	H^{5a}	H^{6a}	H^{OMe}/ H^{Phta1}	H^{Phta2}
$(\mathbf{L^{NH2}})^{2-}$	Ligand	7.58	4.41	3.98	3.74	3.80	3.17		
	1:1	7.70	4.48	4.02	3.79	3.83	3.22		
	1:2	7.72	4.51	4.02	3.76	3.82	3.20		
	1:3	7.65	4.49	4.01	3.74	3.81	3.14		
$(\mathbf{L^{OH}})^{2-}$	Ligand	7.49	4.30	3.85	3.56, 3.49	3.58	3.65		
	1:1	7.55, 7.40	4.33	3.86	3.56, 3.49	3.58	3.66		
	1:2	7.56, 7.41	4.34	3.86	3.56, 3.49	3.58	3.66		
	1:3	7.56	4.34	3.88	3.56, 3.49	3.58	3.66		
$(\mathbf{L^{OMe}})^{2-}$	Ligand	7.43	4.25	3.83	3.63, 3.56	3.52	3.43	3.20	
	1:1	7.55	4.32	3.85	3.65, 3.57	3.53	3.46	3.21	
	1:2	7.56	4.34	3.85	3.65, 3.57	3.52	3.44	3.20	
	1:3	7.48	4.31	3.85	3.64, 3.57	3.52	3.45	3.20	
$(\mathbf{L^{Phta}})^{2-}$	Ligand	7.44	4.21	3.82	3.65, 3.62	3.42	3.60	7.42/7.24	7.31/7.24
	1:1	7.47	4.29	3.82	3.56, 3.62	3.44	3.17	7.52/7.19	7.35/7.32
	1:2	7.45	4.22	3.83	3.66, 3.63	3.41	3.60	7.46/7.24	7.28/7.24
	1:3	7.43	4.27	3.83	3.66, 3.63	3.42	3.61	7.42/7.25	7.31/7.25

Table 4. Ligand-Centered Absorption and Emission Properties of the Free Ligands and of Their $[La(L)_3]^{3-}$ Complexes 3.3×10^{-5}M in Tris-HCl Buffer

			$\tau(^3\pi\pi^*)/\mu$s (77K)τ	
Ln	$E(\pi\rightarrow\pi^*)/cm^{-1}$[a] ($10^{-3}\varepsilon/M^{-1}cm^{-1}$)	$E(^3\pi\pi^*)/cm^{-1}$[b]	τ	%
$(\mathbf{L^{NH2}})^{2-}$	45 455 (12.0), 43 290 (sh, 9.5), 37 453 (sh, 2.1)	25 510, *24 570*	85(6)	38
			242(20)	62
$[La(\mathbf{L^{NH2}})_3]^{3-}$	44 843 (13.0), 41 841 (sh, 8.5), 36 765 (sh, 2.0)	26 810, 25 413, *24 125*, 22 910, 22 099	112(17)	33
			254(15)	67
$(\mathbf{L^{OH}})^{2-}$	45 455 (11.9), 36 630 (2.3)	25 253, *23 866*, 21 739	70(5)	55
			353(9)	45
$[La(\mathbf{L^{OH}})_3]^{3-}$	45 045 (12.4), 41 667 (sh, 5.5), 36 630 (2.3)	27 100, 25 381, *23 810*	85(8)	44
			454(32)	56
$(\mathbf{L^{OMe}})^{2-}$	45 872 (10.4), 43 103 (sh, 5.7), 37 175 (sh, 1.2)	27 027, 26 316, 25 510, *24 038*, 23 310, 21 739	72(6)	36
			353(26)	64
$[La(\mathbf{L^{OMe}})_3]^{3-}$	45 249 (12.4), 42 017 (sh, 6.9), 36 900 (sh, 1.7)	26 810, 25 445, *24 096*	89(3),	58
			475(7)	42
$(\mathbf{L^{Phta}})^{2-}$	45 454 (12.9), 42 553 (sh, 9.1), 36 765 (sh, 2.1)	25 510, *24 096*, 22 676	63(1)	55
			332(11)	45
$[La(\mathbf{L^{Phta}})_3]^{3-}$	45 045 (13.2), 42 017 (sh, 9.1), 36 900 (sh, 2.0)	25 189, *24 331*	63(3)	55
			315(14)	45

[a] From electronic spectra at 298 K, energies are given for the maxima of the band envelopes (sh: shoulder). [b] From phosphorescence spectra at 77 K (water/glycerol 90:10 v/v), the more intense component is italicized.

ethylene arm is not conjugated with the pyridine ring, small electronic effects would be expected upon coordination, leading to small chemical shift differences. Although this trend is respected, the chemical shift differences remain noticeable for the H^1 protons, with $\Delta\delta = 0.06-0.09$ ppm. The $\Delta\delta$ values then decrease expectedly from H^2 to H^6. As for the free ligands, ROESY experiments on the Lu^{III} tris complexes do not evidence NOE effects between the oxyethylene groups and CAChe predictive model calculations confirm that the pendant arms are most likely in an extended conformation.

Ligand-Centered Photophysical Properties. The absorption spectra of the deprotonated ligands feature two main bands located around 220 (45 450 cm^{-1}) and 270 nm (36 360 cm^{-1}), mainly involving orbitals located on the pyridine ring and carbonyl functions. At 295 K, UV excitation in the $\pi \rightarrow \pi^*$ absorption bands of the ligands results in ligand-centered emission displaying one broadband with a maximum around 24 000 cm^{-1}, which is similar to the one observed at 77 K and upon enforcement of a time delay, whatever the ligand is. This band is therefore assigned to emission from a ligand $^3\pi\pi^*$ state (Table 4 and Table S1 in the Supporting Information). This points to efficient intersystem crossing (isc) for all ligands at low temperature. Furthermore, the terminal group of the polyoxyethylene chain influences only marginally the triplet-state energy. Upon complexation with Ln^{III} ions, the absorption maxima undergo slight bathochromic shifts. The latter are on the order of 400 to 800 cm^{-1} for the more energetic absorption band, increasing with the increase in charge density of the cation and concomitant with an increase in the molar absorption coefficient of about 10%. However, the less energetic absorption band is less affected, with bathochromic shifts between 0 and 700 cm^{-1} and no intensity change. The triplet-state energy is also little influenced by the complexation, except for the chelates with $(\mathbf{L^{NH2}})^{2-}$, which show a relatively constant red-shift of about 440−530 cm^{-1}. Vibronic progression is around 1200−1500 cm^{-1}, which is typical of a ring breathing mode. The luminescence decays of the triplet states are biexponential, with a shorter lifetime in the range 60−85 ms (population $\approx {}^1/_3$) and a longer one in the range 240−350 ms (population $\approx {}^2/_3$) for the complexed ligands, both lifetimes are somewhat lengthened in the La^{III} and Lu^{III} complexes.

Lanthanide-Centered Photophysical Properties. The tris chelates formed with europium and terbium ions mainly display the characteristic sharp bands corresponding to the metal-centered emission from the $Eu(^5D_0)$ and $Tb(^5D_4)$ excited states upon ligand excitation at 279 nm. The spectra

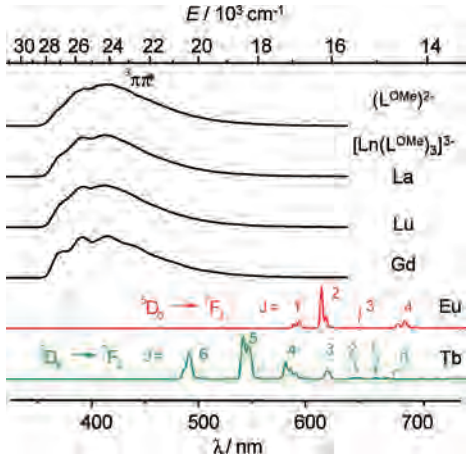

Figure 5. Phosphorescence spectra of $(\mathbf{L^{OMe}})^{2-}$ and its Ln^{III} complexes at 77 K, $[H_2\mathbf{L^{OMe}}]_t = 10^{-4}$ M in Tris-HCl 0.1 M + 10% glycerol, pH 7.4, $\lambda_{exc} = 279$ nm, time delay = 50 μs.

obtained with $\mathbf{H_2L^{OMe}}$ are displayed in Figure 5, whereas those for the other ligands are reported on Figures S8−S10 in the Supporting Information. Only small residual emission from the triplet state is detected: at room temperature it is only seen for the Tb^{III} complex with $(\mathbf{L^{NH2}})^{2-}$ (1% of the total luminescence), whereas at 77 K the triplet state emission accounts for about 6% for the Eu^{III} complex and about 10% for the Tb^{III} complex. Similar values are obtained for the chelates with $(\mathbf{L^{OMe}})^{2-}$ and $(\mathbf{L^{OH}})^{2-}$, whereas ligand phosphorescence makes up 18% of the total light emitted by $[Eu(\mathbf{L^{Phta}})_3]^{3-}$, pointing to a less efficient ligand-to-metal energy transfer.

The overall shape of the luminescence spectra of the Eu^{III} complexes is compatible with a metal ion lying in a coordination site with a pseudo tricapped trigonal prismatic geometry. The magnetic dipole transition $^5D_0 \rightarrow {}^7F_1$ is split into two main components ($A_1 \rightarrow A_2$ and $A_1 \rightarrow E$ in trigonal symmetry), the $^5D_0 \rightarrow {}^7F_2$ transition is dominated by two strong components, and at least five peaks are detected for the $^5D_0 \rightarrow {}^7F_4$ transition. This pattern is in agreement with a geometry derived from D_3 symmetry around the Eu^{III} ion, as reported for $[Eu(dpa)_3]^{3-}$.[14,61,62] In addition, both the relative intensities of the $^5D_0 \rightarrow {}^7F_J$ transitions and the energies of the ligand-field sublevels determined for the $[Eu(L)_3]^{3-}$ complexes are similar to those found for $[Eu(dpa)_3]^{3-}$ (Table S2 in the Supporting Information). This points to an analogous arrangement of the donor atoms in the inner coordination sphere for all the tris complexes investigated here.

The luminescence decays are monoexponential functions for all the Eu^{III} and Tb^{III} complexes. The lifetime of the $Eu(^5D_0)$ level is in the range of 1.36 to 1.47 ms (Table 5) and reflects the absence of water interaction in the inner coordination sphere. At 77 K, these lifetimes are somewhat longer (around 1.8 ms), pointing to the presence of some vibrational quenching processes of the $Eu(^5D_0)$ level by the ligand backbone at room temperature. This is confirmed for $Tb(^5D_4)$ lifetimes, which amount to $\tau \approx 1.4 - 1.5$ ms at 77 K compared to $\tau \approx 1.0 - 1.25$ ms at room temperature, with the exception of $[Tb(\mathbf{L^{NH2}})]^{3-}$, for which $\tau = 1.58$ ms and is temperature independent. To find out whether or not water interacts in the first coordination sphere, hydration numbers have been determined by measuring the lifetimes in deuterated water and using the phenomenological equations of Supkowski and Horrocks for Eu^{III} [63] and of Beeby et al. for Tb^{III}.[64] The results gathered in Table 5 clearly demonstrate the absence of water molecule in the first coordination sphere of all of the Eu^{III} complexes.

In the case of the Tb^{III} chelates, straight application of the phenomenological equations yielded q values between 0.4 and 2.2, very different from those for the Eu^{III} complexes. Similar situations have recently been documented,[52,53] and it was concluded that the failure of the phenomenological equations to predict a correct hydration number was due to the presence of other important nonradiative deactivation processes taking place in the molecular edifices. While in the literature cases[52,53] it was obvious that the basis hypotheses for establishing the phenomenological equations were not met in that energy back transfer was occurring and inducing a dramatic temperature dependence of the $Tb(^5D_4)$ lifetime, this is seemingly not the case here where the room temperature $^5D_4$ lifetime is relatively long and the temperature dependence is not very large. Nevertheless, when 77 K values are taken into account (for both water and deuterated water solutions), the calculated hydration numbers are more similar to those of the Eu^{III} compounds with, possibly, the exception of $[Tb(\mathbf{L^{OH}})]^{3-}$ and $[Tb(\mathbf{L^{Phta}})]^{3-}$, the hydration numbers of which are larger by 0.5 units compared to the corresponding Eu^{III} complexes.[65] Looking at Figure 5, it is obvious that there would be an overlap between the phosphorescence spectrum of the ligand triplet state and the $^5D_4 \leftarrow {}^7F_6$ absorption of the Tb^{III} ion (compare the $^5D_4 \rightarrow {}^7F_6$ emission), which would allow back transfer onto the ligand and could explain the q values determined from room-temperature data. On the other hand, this situation does not occur for Eu^{III}. The case of the $[Tb(\mathbf{L^{OH}})_3]^{3-}$ is noteworthy in that the $Tb(^5D_4)$ level displays the shortest lifetimes of the series and $q \approx 0.5$. Therefore, some second sphere interaction (either intra- or intermolecular) with the hydroxo polyoxyethylene substituent could be envisaged, although this would be at variance with the ROESY experiments conducted on the Lu^{III} chelate. Summarizing the above-discussed data, the nature of the polyoxyethylene substituent does not influence much the lifetime of the $Eu(^5D_0)$ level, which is by far not the case for the $Tb(^5D_4)$ level.

The quantum yields of all the solutions, determined with respect to $Cs_3[Ln(dpa)_3]$ (Ln = Eu, Tb)[27] are reported in Table 5 and show a marked dependence on both the nature of the pendant arm and of the metal ion. The quantum yields

(61) Kim, J. G.; Yoon, S. K.; Sohn, Y.; Kang, J. G. *J. Alloys Compd.* **1998**, *274*, 1–9.
(62) Puntus, L. N.; Zolin, V. F.; Babushkina, T. A.; Kutuza, I. B. *J. Alloys Compd.* **2004**, *380*, 310–314.
(63) Supkowski, R. M.; Horrocks, W. D., Jr. *Inorg. Chim. Acta* **2002**, *340*, 44–48.
(64) Beeby, A.; Clarkson, I. M.; Dickins, R. S.; Faulkner, S.; Parker, D.; Royle, L.; de Sousa, A. S.; Williams, J. A. G.; Woods, M. *J. Chem. Soc., Perkin Trans. 2* **1999**, 493–503.
(65) Note that this procedure has not been validated yet by a series of experimental data and that caution must be exercised when using it.

Table 5. Lifetimes of the $Eu^{III}(^5D_0)$ and $Tb^{III}(^5D_4)$ Levels for 1:3 Ln/L Solutions with $[L]_t = 3 \times 10^{-4}$ M; Hydration Numbers q, Absolute and Intrinsic Quantum Yields, and Ligand Sensitization Efficacies are also given

	τ^a in H_2O/ ms		τ in D_2O/ ms		q^b	Q_{Ln}^{Ld}	$Q^{Ln}{}_{Ln}^{e}$	η_{sens}
	295 K	77 K	295 K	77 K		%	%	%
$[Eu(\mathbf{L^{OH}})_3]^{3-}$	1.36(1)	1.76(3)	2.15(1)	2.54(1)	0.0	11.8(5)	36	33
$[Tb(\mathbf{L^{OH}})_3]^{3-}$	0.99(1)	1.40(2)	2.04(0)	1.83(2)	0.5 [c]	17.8 (6)		
$[Eu(\mathbf{L^{OMe}})_3]^{3-}$	1.36(2)	1.82(1)	2.23(1)	2.52(1)	0.0	26.6(6)	38	70
$[Tb(\mathbf{L^{OMe}})_3]^{3-}$	1.25(2)	1.51(2)	1.69(1)	1.69(1)	0.1[c]	12.7(4)		
$[Eu(\mathbf{L^{NH2}})_3]^{3-}$	1.43(1)	1.82(1)	2.20(1)	2.58(2)	0.0	28.9(9)	40	72
$[Tb(\mathbf{L^{NH2}})_3]^{3-}$	1.58(2)	1.59(1)	1.91(1)	1.73(1)	−0.1[c]	15.3(5)		
$[Eu(\mathbf{L^{Phta}})_3]^{3-}$	1.47(1)	1.85(1)	1.95(2)	2.57(1)	−0.1	18.3(4)	42	44
$[Tb(\mathbf{L^{Phta}})_3]^{3-}$	1.08(2)	1.51(2)	1.95(2)	1.87(1)	0.3[c]	10.8(4)		
$[Eu(\mathbf{dpaOMe})_3]^{3-}$	1.36(1)	2.57(1)	2.01(2)	2.94(2)	0.1	16.1(7)	36	45
$[Tb(\mathbf{dpaOMe})_3]^{3-}$	1.80(1)	1.93(7)	2.51(1)	2.11(3)	0.2	14.5(6)		
$[Eu(\mathbf{dpa})_3]^{3-}$	1.67(3)[e]		3.0(1)[e]		0.0	24(2.5)[e]	39	61
$[Tb(\mathbf{dpa})_3]^{3-}$	1.41(1)	2.07(1)	2.35(2)	2.27(1)	0.2	22(2.5)		

[a] Analysis on the $^5D_0 \rightarrow {}^7F_2$ (Eu^{III}) and $^5D_4 \rightarrow {}^7F_5$ (Tb^{III}) transitions. [b] ±0.3; determined according to the equations of Supkowski[63] and Beeby[64] (average, Eu^{III}), and Beeby[64] (Tb^{III}), uncertainty is ± 0.3. [c] At 77 K (see text) [d] For solutions with $A = 0.2$, $\lambda_{exc} = 279$ nm, ± 10%. [e] From ref 27.

of the Eu^{III} chelates range between 12 and 29%, whereas those for Tb^{III} complexes are significantly smaller, ranging between 11 and 18%. Moreover, the sequence is different for both ions, the quantum yields decreasing in the series $[Eu(\mathbf{L^{NH2}})_3]^{3-} > [Eu(\mathbf{L^{OMe}})_3]^{3-} > [Eu(\mathbf{L^{Phta}})_3]^{3-} > [Eu(\mathbf{L^{OH}})_3]^{3-}$ for europium and $[Tb(\mathbf{L^{OH}})_3]^{3-} > [Tb(\mathbf{L^{NH2}})_3]^{3-} > [Tb(\mathbf{L^{OMe}})_3]^{3-} > [Tb(\mathbf{L^{Phta}})_3]^{3-}$ for terbium, pointing to $(\mathbf{L^{OH}})^{2-}$ being the best sensitizer of the terbium luminescence and the less efficient one for europium emission. The overall quantum yield Q_L^{Ln} of a lanthanide coordination compound is the product of the intrinsic quantum yield Q_{Ln}^{Ln} (measured upon f−f excitation), which reflects the extent of nonradiative deactivation processes taking place within the luminescent edifice, and the sensitization efficiency of the ligand (η_{sens}), which reflects the efficacy with which the latter transfers its excitation energy onto the metal ion. In the case of Eu^{III}, simple equations allow one to determine the otherwise difficult-to-measure Q_{Eu}^{Eu} yield from spectral parameters and lifetimes:[66]

$$Q_L^{Eu} = \eta_{sens} \times Q_{Eu}^{Eu} \tag{7}$$

where η_{obs} and η_{rad} are the observed and radiative lifetimes, respectively; the latter is calculated from:

$$1/\tau_{rad} = 14.65(I_{tot}/I_{MD})n^3[s^{-1}] \tag{8}$$

where I_{tot}/I_{MD} is the ratio of the total emitted intensity to the intensity of the magnetic dipole transition $^5D_0 \rightarrow {}^7F_1$. We found that, in all cases, including the parent dpa^{2-} chelate and the comparison complex with $(\mathbf{dpaOMe})^{2-}$, the intrinsic quantum yields Q_{Eu}^{Eu} are very similar, within experimental errors, ranging between 36 and 42% (Table 5). That is, substitution of the polyoxyethylene arm does not affect appreciably the deactivation processes within the triple helical structures. Therefore, differences in the overall quantum yields essentially arise from differences in the sensitization efficiency η_{sens} provided by the ligands. With respect to the parent dpa^{2-} tris chelate (61%), $(\mathbf{L^{OMe}})^{2-}$ and $(\mathbf{L^{NH2}})^{2-}$ are slightly better sensitizers, with $\eta_{sens} \approx 70\%$, whereas the two others and the comparison ligands transfer energy much less efficiently with $\eta_{sens} \approx 33-45\%$. This points to a remarkable fine-tuning of the photophysical properties of the europium triple-helical chelates by the terminal functional group of the polyoxyethylene substituent, the overall quantum yield increasing by a factor 2.4 between the chelates with $(\mathbf{L^{OH}})^{2-}$ and $(\mathbf{L^{NH2}})^{2-}$. The tuning for Tb^{III} chelates is less remarkable, the improvement factor between $[Tb(\mathbf{L^{Phta}})_3]^{3-}$ and $[Tb(\mathbf{L^{OH}})_3]^{3-}$ being only 1.6 fold. Another interesting point is the large decrease in quantum yield consecutive to the introduction of a methoxy group on the pyridine 4-position of dipicolinic acid, which amounts to 30% in going from $[Ln(\mathbf{dpa})_3]^{3-}$ to $[Ln(\mathbf{dpaOMe})_3]^{3-}$ for both Eu^{III} and Tb^{III}. These data are in line with the quantum yield published by Latva et al. for the tris chelate with 4-(naphthalen-2-yloxy)-pyridine-2,6-dicarboxylate having $Q_L^{Eu} = 12\%$ (recalculated with $Q([Ln(dpa)_3]^{3-}) = 24\%$[27] instead of 13% [46]). For the ligands presented in this article, the detrimental effect of ether substitution in the para position of the pyridine moiety is apparently compensated by the presence of the terminal X substituent on the polyoxyethylene arm, at least for X = OMe and NH_2 and, less efficiently, for X = Phta, whereas the alcohol group has no positive effect. As far as the phtalimide group is concerned, no enhanced antenna effect is observed, within experimental errors, over the $(\mathbf{dpaOMe})^{2-}$ ligand, which is consistent with this chromophoric unit lying too far from the metal center for contributing in a sizable way to the energy-transfer process. As far as terbium chelates are concerned, a detailed discussion is more difficult in absence of η_{sens} data and because of the more complex contribution from nonradiative deactivation processes.

Conclusion

The tris chelates formed with the four new ligands $\mathbf{H_2L^X}$ described here, differing by the terminal substituent of a polyoxyethylene arm grafted on the 4- position of the pyridine ring of dipicolinic acid, are thermodynamically stable at physiological pH and present photophysical properties compatible with their use as bioprobes. The ligands sensitize satisfyingly the Eu^{III} luminescence, as well as the Tb^{III} luminescence, although to a lesser extent. A remarkable tuning of the quantum yield is evidenced depending on the nature of the terminal substituent, at least for the Eu^{III} chelates

(66) Werts, M. H. V.; Jukes, R. T. F.; Verhoeven, J. W. *Phys. Chem. Chem. Phys.* **2002**, *4*, 1542–1548.

for which the quantum yield can be varied from 12% (X = OH) to 29% (X = NH_2); sensitizing efficiencies of the europium-centered luminescence by the ligands are as large as 70% for X = OMe and NH_2, resulting in quantum yield in water at physiological pH around 27−29%, that is larger than the value reported for the parent $[Eu(dpa)_3]^{3-}$ complex (24%). In the case of Tb^{III}, substitution of the pyridine 4-position has always had a detrimental effect on the quantum yields, which range from 11 to 18%, as compared to 22% for $[Tb(dpa)_3]^{3-}$.[27] Simultaneous analysis of the quantum yield and lifetime data evidence a rather intricate situation where nonradiative deactivation may play a prominant role, possibly through energy back transfer owing to the overlap between the ligand triplet state emission and the Tb^{III} absorption spectrum.

It has been claimed that coupling a lanthanide probe to a biological molecule (e.g., a protein) might deactivate its luminescence because of the detrimental proximity of quenching groups,[5] but the nature of the linking has not attracted much consideration so far. The series of complexes described here can be taken as simple models for the formation of chemical bonds between a luminescent probe and a biological target. For instance, the alcohol-substituted ligand $(\mathbf{L^{OH}})^{2-}$ can form an ether bond with a biological target, which is mimicked by $[Eu(\mathbf{L^{OMe}})_3]^{3-}$, for which the sensitization efficiency is greatly enhanced by a factor >2. However, using an amine function to produce an amide linkage by reaction with a carboxylic acid group of the biological target is foreseen to decrease the sensitization of the europium if we accept the idea that the phtalimide substituent can mimic such a carboxamide coupling. The data reported here therefore will help in rationalizing the ligand design of lanthanide biological probes with respect to the expected effect on photophysical properties upon coupling to the biological material. Work is in progress in our laboratory toward this goal.

Experimental Section

General Procedures. Solvents were purified by a nonhazardous procedure by passing them onto activated alumina columns (Innovative Technology Inc. system).[67] Chemical products were ordered from Fluka and Aldrich and used without any further purification. 4-Hydroxy-pyridine-2,6-dicarboxylic acid diethyl ester (**2**) and 4-{2-[2-(2-methoxy-ethoxy)-ethoxy]-ethoxy}-pyridine-2,6-dicarboxylic acid diethyl ester (**4**) have been obtained as previously reported.[53] The 1:3 complexes were synthesized in situ by mixing three eqs of the desired ligand with 1 equiv of $Ln(ClO_4)_3 \cdot xH_2O$ (Ln = La, Lu, Gd, Tb, Eu, $x = 2.5-4.5$) in water or, when needed, in a Tris-HCl 0.1 M buffer solution (pH = 7.4).

Caution! *Perchlorate salts combined with organic compounds are potentially explosive and should be handled in small quantities and with adequate precautions.*[68]

^{1}H-NMR spectra were performed on a Bruker Avance DRX 400 spectrometer and ^{13}C NMR spectra on a Bruker AV 600 MHz at 25 °C, using deuterated solvents as internal standards. ESI-MS spectra were obtained on a Finnigan SSQ 710C spectrometer using 10^{-5} to 10^{-4} M solutions in acetonitrile/H_2O/acetic acid (50:50:1) or MeOH, capillary temperature 200 °C, and acceleration potential 4.5 keV. The instrument was calibrated using horse myoglobin standard and analyses were conducted in positive mode with a 4.6 keV ion spray voltage. Elemental analyses were performed by Dr. Solari at the École Polytechnique Fédérale de Lausanne. UV−vis spectra were measured in 0.2 cm quartz Suprasil cuvettes on a PerkinElmer Lambda 900 spectrometer. Molecular modeling was performed with the CAChe workpackage 7.5 (Fujitsu, 2000−2006).

Physicochemical Measurements. Protonation constants of the ligands were determined with the help of a J&M diode array spectrometer (Tidas series) connected to an external computer. All titrations were performed in a thermostatted (25.0 ± 0.1 °C) glass-jacketed vessel at μ = 0.1 M (KCl). In a typical experiment 50 mL of a ligand solution 10^{-4} M were titrated by freshly prepared sodium hydroxide solutions at different concentrations (10, 4, 1, 0.1, and 0.01 M). After each addition, the pH of the solution was measured by a KCl-saturated electrode (Methrom Nr. 6.0224 100) and the UV−vis absorption spectrum was recorded using a 1 cm Hellma optrode immersed in the thermostatted titration vessel. Measurements were conducted in the pH range 1.1−12. Using the same equipment, conditional stability constants were determined by titration of the ligands 10^{-4} M by Ln^{III} 5×10^{-3} M (Ln = La, Eu, Lu) at fixed pH 7.4 (0.1 M Tris-HCl buffer). Factor analysis[69] and mathematical treatment of the spectrophotometric data were performed with the *Specfit* software.[70,71] Broadband excited emission spectra were recorded in photon-counting mode on a Fluorolog FL-3−22 spectrometer from Horiba-Jobin-Yvon Ltd.; quartz cells with optical paths of 0.2 cm were used for room-temperature spectra, whereas 77 K measurements were carried out on samples put into quartz Suprasil capillaries. All spectra are corrected for the instrumental function. Quantum yields were determined in aerated water with respect to $[Ln(dpa)_3]^{3-}$ (Ln = Eu, Q = 24%, Ln = Tb, Q = 22%).[27] Absorbance of the samples and reference was measured three times and at three different absorbance values (≈ 0.1, ≈ 0.15, and ≈ 0.2).

Syntheses of the ligands (see Scheme 2). 4-{2-[2-(2-Methoxy-ethoxy)-ethoxy]-ethoxy}-pyridine-2,6-dicarboxylic Acid ($H_2\mathbf{L^{OMe}}$). A solution of NaOH (456 mg, 11.4 mmol) in 50 mL of water was added to **4** (2 g, 5.2 mmol), suspended in water (50 mL), and the resulting solution was stirred at room temperature for 2 h. The evolution of the reaction was followed by TLC (silica plate, CH_2Cl_2/MeOH 97:3 v/v). After completion of the reaction, the basic aqueous solution was washed with 2 × 50 mL CH_2Cl_2, acidified until pH 2.0 with HCl 0.1 M, and the aqueous phase was evaporated. The crude product (1.8 g) was purified by chromatography (reverse-phase, MeCN, H_2O, TFA 0.05%) to give $H_2\mathbf{L^{OMe}}$ as a pale-yellow solid. Yield 1.45 g, 85%. Anal. Calcd for $C_{14}H_{19}NO_8 \cdot 0.35\ H_2O$ (%): C, 50.10; H, 5.92; N, 4.17. Found: C, 50.12; H, 6.40; N,4.20. ^{1}H NMR (D_2O): 7.70 (s, 2H, H_{ar}), 4.47 (s, 2H, H^1), 4.01 (s, 2H, H^2), 3.81 (d, ^3J = 3.48 Hz and d, ^3J = 4.39 Hz, 2H, $H^{3,4}$), 3.75 (d, ^3J = 3.48 Hz and d, ^3J = 4.39 Hz, 2H, $H^{3,4}$), 3.71 (d, ^3J = 4.94 Hz and d, ^3J = 3.66 Hz, 2H, $H^{5,6}$), 3.61 (d, ^3J = 4.94 Hz and d, ^3J = 3.66 Hz, 2H, $H^{5,6}$), 3.40 (s, 3H, OCH_3). ^{13}C NMR (D_2O): 173.47 (C═O), 162.89 (C−O), 146.71 (C_{ar}), 114.76 (CH_{ar}), 70.94 (OCH_2), 69.91 (OCH_2), 69.82 (OCH_2), 69.48 (OCH_2), 69.42 (OCH_2), 68.22 (OCH_2), 35.12 (OCH_3). ESI-MS: found 330.30 $(M+H)^+$ (Calcd 330.31).

(67) Pangborn, A. B.; Giardello, M. A.; Grubbs, R. H.; Rosen, R. K.; Timmers, F. J. *Organometallics* **1996**, *15*, 1518–1520.
(68) Raymond, K. N. *Chem. Eng. News* **1983**, *61*, 4.
(69) Malinowski,E. R.; Howery,D. G. *Factor Analysis in Chemistry*; John Wiley: New York, Chichester, Brisbane, Toronto, 1991.
(70) Gampp, H.; Maeder, M.; Meyer, C. J.; Zuberbühler, A. D. *Talanta* **1985**, *32*, 257–264.
(71) Gampp, H.; Maeder, M.; Meyer, C. J.; Zuberbühler, A. D. *Talanta* **1986**, *33*, 943–951.

4-{2-[2-(2-Hydroxyethoxy)ethoxy]ethoxy}pyridine-2,6-dicarboxylic Acid Diethyl Ester (5). To a solution of **4** (1 g, 2.59 mmol) dissolved in MeCN (70 mL) was added dropwise TMSI (0.7 mL, 5.18 mmol). The brown solution was refluxed for 6 h, then left to return to room temperature. Methanol was added (10 mL) and then solid $Na_2S_2O_3$ until the solution turned bright yellow. The solvents were evaporated and the crude product redissolved in dichloromethane, giving a precipitate that was discarded. This treatment was repeated until no precipitation occurred. The solvent was evaporated and the product was purified by chromatography (silica gel, MeOH/CH_2Cl_2, 98:2 v/v) to give **5** as a pale-yellow oil. Yield: 0.78 g, 81%. ^{1}H NMR ($CDCl_3$): 7.78 (s, 2H, H_{ar}), 4.44 (q, ^3J = 7.01 Hz, 2H, $OC\underline{H}_2CH_3$), 4.28 (d, ^3J = 4.68 Hz, 2H, H^1), 3.88 (d, ^3J = 4.68 Hz, 2H, H^2), 3.70 (m, 4H, H^5 and H^6), 3.69 (m, 2H, $H^{3,4}$), 3.57 (m, 2H, $H^{3,4}$), 1.41 (t, ^3J = 7.01 Hz, 3H, $OCH_2C\underline{H}_3$). ^{13}C NMR ($CDCl_3$): 166.82 (C═O), 164.71 (C−O), 150.24 (C_{ar}), 114.41 (CH_{ar}), 72.48 (OCH_2), 71.00 (OCH_2), 70.41 (OCH_2), 69.18 (OCH_2), 68.23 (OCH_2), 62.38 ($O\underline{C}H_2CH_3$), 61.77 (OCH_2), 14.18 ($OCH_2\underline{C}H_3$). ESI-MS: found 372.32 $(M+H)^+$ (Calcd 372.15).

Disodium 4-{2-[2-(2-hydroxyethoxy)ethoxy]ethoxy}pyridine-2,6-dicarboxylate Na_2L^{OH}. A solution of NaOH (170 mg, 4.2 mmol) in 50 mL of water was added to **5** (0.78 g, 2.1 mmol) suspended in water (50 mL), and the resulting solution was stirred at room temperature for 2 h. The evolution of the reaction was followed by TLC (silica plate, CH_2Cl_2/MeOH 97:3 v/v). After completion of the reaction, the basic aqueous solution was washed with 2 × 50 mL CH_2Cl_2, and the aqueous phase was evaporated. The crude product (1.8 g) was purified by chromatography (silica gel, MeCN, NH_4OAc, 100 → 75:25 v/v) to give $Na_2\mathbf{L}^{\mathbf{OH}}$ as a pale-yellow solid. Yield: 0.62 g, 82%. Anal. Calcd for $C_{13}H_{15}NO_8Na_2$ 3 NaOH: C, 32.58; H, 3.79; N, 2.92. Found: C, 32.54; H, 3.45; N, 2.47. ^{1}H NMR (D_2O): 7.54 (s, 2H, H_{ar}), 4.34 (t, ^3J = 4.17 Hz, 2H, H^1), 3.93 (t, ^3J = 4.17 Hz, 2H, H^2), 3.74 (d, ^3J = 6.56 Hz and d, J = 4.77 Hz, 2H, $H^{5.6}$), 3.68 (d, ^3J = 6.56 Hz and d, J = 4.77 Hz, 2H, $H^{5.6}$), 3.66 (t, ^3J = 4.97 Hz, 2H, $H^{3.4}$), 3.58 (t, ^3J = 4.97 Hz, 2H, $H^{3.4}$). ^{13}C NMR (D_2O): 172.88 (C═O), 166.96 (C−O), 155.21 (C_{ar}), 111.87 (CH_{ar}), 72.83 (OCH_2), 70.21 (OCH_2), 69.78 (OCH_2), 69.07 (OCH_2), 67.82 (OCH_2), 60.68 (CH_2OH). ESI-MS: found 316.28 $(M+H)^+$ (Calcd 316.29).

2-{2-[2-(2-Methoxy-ethoxy)-ethoxy]-ethyl}-isoindole-1,3-dione (6). To a solution of **3** (5.6 g, 33.5 mmol) in thf (200 mL) were added triphenyl phosphine (8.9 g, 33.5 mmol) and phtalimide (5 g, 33.5 mmol). Azodicarboxylic acid diisopropyl ester DIAD (6.9 g, 33.5 mmol) was then slowly added under stirring, and the solution was refluxed overnight. The solvent was evaporated, the crude product was dissolved in 150 mL of petroleum ether/ethyl acetate 1:1, and left at 4 °C for 1 h, during which white triphenylphenyloxide precipitated. After filtration, the filtrate was evaporated to give a brown oil, which was purified by chromatography (silica gel, EtOAc) to provide the desired product as a pale-yellow oil. Yield: 4.0 g, 84%. ^{1}H NMR ($CDCl_3$): 7.83 (dd, ^3J = 5.26 Hz and ^4J = 2.34 Hz, 2H, H_{ar}), 7.72 (dd, ^3J = 5.26 Hz and ^4J = 2.34 Hz, 2H, H_{ar}), 3.90 (t, ^3J = 5.85 Hz, 2H, H^1), 3.74 (t, ^3J = 5.85 Hz, 2H, H^2), 3.65 (d, ^3J = 5.26 and d, ^3J = 4.97 Hz, 2H, $H^{3.4}$), 3.60 (d, ^3J = 6.43 and d, ^3J = 4.97 Hz, 2H, $H^{5.6}$), 3.57 (d, ^3J = 5.26 and d, ^3J = 4.97 Hz, 2H, $H^{3,4}$), 3.47 (d, ^3J = 6.43 and d, ^3J = 4.97 Hz, 2H, $H^{5.6}$), 3.34(s, 3H, OCH_3). ESI-MS: found 294.34 $(M+H)^+$ (Calcd 294.13).

2-{2-[2-(2-Hydroxy-ethoxy)-ethoxy]-ethyl}-isoindole-1,3-dione (7). To a solution of **6** (2 g, 6.8 mmol) dissolved in MeCN (50 mL) was added dropwise TMSI (1.9 mL, 13.6 mmol). The solution was heated at 70 °C for 2 h under nitrogen atmosphere then left to return to room temperature. Methanol was added (20 mL), and the solvents were evaporated. The crude product was redissolved in dichloromethane and washed with an aqueous solution of $Na_2S_2O_3$ 0.5 M. The organic phase was dried over Na_2SO_4 and evaporated. The product was pure enough to be directly used in the next step (orange oil). Yield: 1.9 g, 98%. ^{1}H NMR ($CDCl_3$): 7.85 (dd, ^3J = 5.55 Hz and ^4J = 2.93 Hz, 2H, H_{ar}), 7.72 (dd, ^3J = 5.55 Hz and ^4J = 2.93 Hz, 2H, H_{ar}), 3.91 (t, ^3J = 5.57 Hz, 2H, H^1), 3.75 (t, ^3J = 5.57 Hz, 2H, H^2), 3.65 (m, 4H, $H^{3,4}$ + $H^{5.6}$), 3.37 (d, ^3J = 6.36 Hz and d, ^3J = 4.97 Hz, 2H, $H^{3,4}$), 3.53 (d, ^3J = 4.38 and d, ^3J = 4.57 Hz, 2H, $H^{5.6}$). ^{13}C NMR ($CDCl_3$): 168.34 (C═O), 133.97 (CH_{ar}), 132.07 (C_{ar}), 123.30 (CH_{ar}), 76.79 (OCH_2), 72.41 (OCH_2), 70.34 (OCH_2), 67.92 (OCH_2), 61.75 (OCH_2), 37.16 (NCH_2). ESI-MS: found 279.33 (M^+) (Calcd 279.11).

4-(2-{2-[2-(1,3-Dioxo-1,3-dihydro-isoindol-2-yl)-ethoxy]-ethoxy}-ethoxy)-pyridine-2,6-dicarboxylic Acid Diethyl Ester (8). To a solution of **2** (0.5 g, 2.2 mmol) in thf (150 mL) were added triphenyl phosphine (0.85 g, 3.2 mmol) and **7** (0.9 g, 3.2 mmol). Azodicarboxylic acid diisopropyl ester DIAD (0.65 g, 3.2 mmol) was then slowly added under stirring, and the solution was heated at 70 °C overnight. The solvent was evaporated, the crude product was dissolved into 150 mL of petroleum ether/ethyl acetate 1:1 and left at 4 °C for 1 h, during which white triphenylphenyloxide precipitated. After filtration, the filtrate was evaporated to give an oil, which was purified by chromatography (silica gel, EtOAc) to provide the desired product as a pale-yellow oil. Yield: 0.8 g, 76%. ^{1}H NMR ($CDCl_3$): 7.82 (m, 2H, H_{Phta}), 7.75 (s, 2H, H_{py}), 7.69 (m, 2H, H_{Phta}), 4.46 (q, ^3J = 7.24 Hz, 6H, $OC\underline{H}_2$-CH_3), 4.19 (t, ^3J = 4.82 Hz, 2H, H^1), 3.90 (m, 4H, H^2 and $H^{3,4}$), 3.82 (t, ^3J = 4.39 Hz, 2H, $H^{3,4}$), 3.74 (t, ^3J = 5.70 Hz, 4H, $H^{5.6}$), 4.46 (t, ^3J = 7.24 Hz, 4H, $OC\underline{H}_2-CH_3$). ^{13}C NMR ($CDCl_3$): 168.22 (C═O_{py}), 167.72 (C−O_{py}), 164.66 (C−O_{Phta}), 150.13 (C_{py}), 133.93 (CH_{Phta}), 132.10 (CH_{Phta}), 123.19 (CH_{Phta}), 114.36 (CH_{py}), 70.82 (OCH_2), 70.21 (OCH_2), 69.10 (OCH_2), 68.22 (OCH_2), 67.99 (OCH_2), 62.33 ($O\underline{C}H_2CH_3$), 32.27 (NCH_2), 14.17 ($OCH_2\underline{C}H_3$). ESI-MS *m*/*z* found for $[M+H^+]$ 501.31 (Calcd 501.18)

Disodium 4-(2-{2-[2-(1,3-dioxo-1,3-dihydro-2H-isoindol-2-yl)ethoxy]ethoxy}ethoxy)pyridine-2,6-dicarboxylate (Na_2L^{Phta}). A solution of NaOH (65 mg, 1.6 mmol) in 50 mL of ethanol was added to **8** (0.3 g, 0.6 mmol) dissolved in ethanol (50 mL), and the resulting solution was stirred at room temperature for 2 h. The evolution of the reaction was followed by TLC (silica plate, CH_2Cl_2/MeOH 97:3 v/v). After completion of the reaction, the ethanol was evaporated and the crude product was purified by chromatography (silica gel, MeCN, NH_4OAc, 100 → 80:20 v/v) to give $Na_2\mathbf{L}^{\mathbf{Phta}}$ as a pale-yellow solid. Yield: 0.24 g, 80%. Anal. Calcd for $C_{21}H_{18}N_2O_9Na_2$ 2 NaOH: C, 42.29; H, 3.50; N, 4.70. Found: C, 42.35; H, 3.26; N, 4.19.^{1}H NMR (NaOD 0.1M): 7.59 (d, 1H, H_{Phta1}), 7.52 (s, 2H, H_{py}), 7.47 (dd, ^3J = 7.35 Hz, ^4J = 1.79 Hz, 1H, H_{Phta2}), 7.39 (m, 2H, $H_{Phta1\,+\,2}$), 4.30 (t, ^3J = 4.37 Hz, 2H, H^1), 3.96 (t, ^3J = 4.37 Hz, 2H, H^2), 3.80 (t, ^3J = 5.37, 2H, H^6), 3.76 (m, 4H, $H^{5.4}$), 3.37 (t, ^3J = 5.37, 2H, H^3). ^{13}C NMR (NaOD 0.1M): 175.72 (C═O_{py}), 173.07 (C═O_{py}), 172.58 (C−O_{py}), 166.42(C−O_{Phta}), 154.81 (C_{py}), 137.47 (CH_{Phta}), 134.33 (CH_{Phta}), 130.25 (CH_{Phta}), 129.29 (CH_{Phta}), 127.95 (CH_{Phta}), 127.03 (CH_{Phta}), 111.38 (CH_{py}), 69.73 (OCH_2), 69.43 (OCH_2), 68.72 (OCH_2), 68.63 (OCH_2), 67.37 (OCH_2), 39.53 (NCH_2).

4-{2-[2-(2-aminoethoxy)ethoxy]ethoxy}pyridine-2,6-dicarboxylic Acid (H_2L^{NH2}). A solution of NaOH (240 mg, 6 mmol) in 50 mL of water was added to **8** (0.3 g, 0.6 mmol) suspended in water (50 mL), and the resulting solution was stirred at room temperature for 2 h. The evolution of the reaction was followed by TLC (silica plate, CH_2Cl_2/MeOH 97:3 v/v). After completion of the reaction, the basic aqueous solution was washed with 2 × 50 mL CH_2Cl_2,

and the aqueous phase was evaporated. The crude product (1.8 g) was purified by chromatography (reverse-phase, MeCN, H_2O, TFA 0.05%) to give $\mathbf{H_2L^{NH2}}$ as a pale-yellow solid (0.14 g, 75%). ^{1}H NMR (400 MHz, D_2O) δ: 7.58 (s, 2H, H_{ar}), 4.41 (m, 2H, H^1), 3.99 (m, 2H, H^2), 3.81 (m, 2H, H^5), 3.73 (m, 2H, H^4), 3.57 (m, 2H, H^3), 2.78 (m, 2H, H^6). ^{13}C NMR (600 MHz, D_2O) $\delta_{(ppm)}$: 174.11 (C═O), 167.93 (C−O), 156.35 (C_{ar}), 112.79 (CH_{ar}), 73.60 (OCH_2), 71.20 (OCH_2), 70.72 (OCH_2), 70.09 (OCH_2), 68.78 (OCH_2), 41.26 (CH_2NH_2). ESI-MS *m*/*z* calc for [M+H$^+$] (found): 315.11 (315.35). Anal. Calcd for $C_{13}H_{18}N_2O_7 \cdot 2.15$ TFA (found): C, 41.52 (41.51); H, 4.38 (4.42); N, 6.37 (6.04).

4-Methoxy-pyridine-2,6-dicarboxylic Acid Dimethyl Ester. Chelidamic acid (0.8 g, 4.4 mmol) was refluxed in methanol (50 mL) in presence of sulfuric acid (1 mL) for 4 days, and the completion of the reaction was checked by mass spectrometry. The solvent was removed, the crude product dissolved in water and neutralized by saturated $NaHCO_3$ solution. It was extracted by dichloromethane, the organic phase dried over $Na_2S_2O_4$ and the solvent evaporated to give 4-methoxy-pyridine-2,6-dicarboxylic acid dimethyl ester (0.6 g, 61%). ^{1}H NMR (400 MHz, $CDCl_3$): 7.80 (s, 2H, H_{ar}), 4.03 (s, 6H, CO_2Me), 3.97 (s, 3H, OMe). ESI-MS: *m*/*z* Calcd for [M+H$^+$] (found): 226.06 (226.34).

4-Methoxy-pyridine-2,6-dicarboxylic acid (H_2dpaOMe). 4-methoxy-pyridine-2,6-dicarboxylic acid dimethyl ester (0.5 g, 2.2 mmol) was dissolved in water (50 mL) in presence of NaOH (200 mg, 5 mmol), and the solution was stirred at room temperature overnight. The aqueous phase was washed with dichloromethane (2 × 50 mL), then the pH lowered with HCl 1 M until formation of a pale-yellow solid, which was collected, rinsed with cold water, and dried under vacuum for 48 h. Yield: 0.35 g, 80%. Anal. Calcd for $C_8H_7NO_5$: C, 48.74; H, 3.58; N, 7.10. Found: C, 48.58; H, 3.61; N, 7.08. ^{1}H NMR (DMSO-*d6*): 7.61 (s, 2H, H_{ar}). ESI-MS: found 198.29 (M+H)$^+$ (Calcd 198.03).

Acknowledgment. This research is supported through a grant from the Swiss National Science Foundation (200020-119866/1). We thank Steve Comby (luminescence) and Frédéric Thomas, Loïc Wagnières and Baptiste Grund (synthesis of the ligands) and for their invaluable assistance.

Supporting Information Available: Table of the absorption and emission data of the ligands and associated tris complexes, table of the ligand-field sublevels of the Eu^{III} tris chelates, figures showing the UV−vis titration of the ligands and corresponding spectra and distribution diagrams, figure of the NMR titration of $(\mathbf{L^{NH2}})^{2-}$ by $Lu(ClO_4)_3$, figures containing the low-temperature phosphorescence spectra of the ligands and their complexes. This material is available free of charge via the Internet at http://pubs.acs.org.

IC800842F